Large Quadratic Nonlinear Optical Efficiencies in Pseudosymmetric Streptocyanine Dyes

Valérie Guieu, Corinne Payrastre,* and Yves Madaule

Laboratoire de Synthèse et Physicochimie de Molécules d'Intérêt Biologique, UMR 5068, Université Paul Sabatier, 31062 Toulouse Cedex 9, France

Sonia Garcia-Alonso

Laboratoire d'Hétérochimie Fondamentale et Appliquée, Université Paul Sabatier, 118 route de Narbonne, 31062 Toulouse, France

Pascal G. Lacroix*

Laboratoire de Chimie de Coordination du CNRS, 205 route de Narbonne, 31077 Toulouse, France

Keitaro Nakatani

PPSM, Ecole Normale Supérieure de Cachan, UMR 8531, 61 Avenue du Pdt Wilson, 94235 Cachan, France

Received March 10, 2006. Revised Manuscript Received May 22, 2006

The quadratic ($\propto E^2$) nonlinear optical (NLO) properties of pseudosymmetric organic cations are investigated. These chromophores belong to a family of highly polarizable streptocyanine dyes built in two steps by amination of their related carboxonium salts. They exhibit a nearly perfect optical transparency in the 200−1100 nm range, except around 700 nm, where a single but narrow band is present. Some of these dyes crystallize in noncentrosymmetric space groups, which, despite a symmetrical π-electronic structure, leads to symmetry lowering and restores a push−pull character to the optical transition and hence a sizable molecular hyperpolarizability. One of these molecules is optimized for a solid-state NLO effect and exhibits an efficiency 120 times that of urea in second harmonic generation at 1.907 μm.

Introduction

The emerging optoelectronic and photonic technologies have stimulated much research of the nonlinear optical (NLO) properties of various molecular materials in relation to their high NLO efficiencies, ultrafast response times, and chemical flexibilities related to the tremendous capabilities of molecular synthetic chemistry.[1,2] Although recent years have witnessed the emergence of promising multipolar (e.g., octupolar) topologies,[2d,3,4] the most traditional approach which guarantees a large molecular hyperpolarizability (β) implies the design of molecular units in which a strong electron acceptor is linked to a strong electron donor through a π-conjugated pathway.[5] This topology is exemplified in Scheme 1 in the case of the benchmark dimethylaminonitrostilbene (DANS) molecule.

Scheme 1

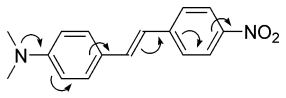

However, besides the design of suitable molecular units, one of the main bottlenecks in the development of efficient molecular NLO materials has been related to the engineering of the molecules into a noncentrosymmetric solid-state environment if the molecular property (β) is to contribute to an observable bulk nonlinear susceptibility ($\chi^{(2)}$). To meet this challenge, an intensively investigated strategy is based on dipole orientation by electric poling of NLO polymers, with the nondesirable outcome of signal decay after long periods of time.[6,7] On the other hand, the most traditional approach toward solid-state NLO efficiency is the crystal

* To whom correspondence should be addressed. E-mail: pascal@lcc-toulouse.fr.

(1) For reviews on NLO properties in organic molecules, see: (a) *Molecular Nonlinear Optics: Materials, Physics and Devices*; Zyss, J., Ed.; Academic Press: New York, 1994. (b) *Nonlinear Optics of Organic Molecules and Polymers*; Nalwa, H. S., Miyata, S., Eds.; CRC Press: Boca Raton, FL, 1997. (c) Delaire, J. A.; Nakatani, K. *Chem. Rev.* **2000**, *100*, 1817.

(2) For reviews on NLO properties in inorganic molecules, see: (a) Di Bella, S. *Chem. Soc. Rev.* **2001**, *30*, 355. (b) Lacroix, P. G. *Eur. J. Inorg. Chem.* **2001**, 339. (c) Coe, B. J. In *Comprehensive Coordination Chemistry 2*, McCleverty, J. A., Meyer, T. J., Eds.; Elsevier Pergamon: Oxford, U.K., 2004; Vol. 9, p 621. (d) Maury, O.; Le Bozec, H. *Acc. Chem. Res.* **2005**, *38*, 691.

(3) For a report exemplifying the 2-D approach, see: Thallapally, P. K.; Desiraju, G. R.; Bagieu-Beucher, M.; Masse, R.; Bourgogne, C.; Nicoud, J.-F. *Chem. Commun.* **2002**, 1052.

(4) For an introduction of NLO properties in octupolar chromophores, see: (a) Zyss, J.; Ledoux, I. *Chem. Rev.* **1994**, *94*, 77. (b) Brunel, J.; Mongin, O.; Jutand, A.; Ledoux, I.; Zyss, J.; Blanchard-Desce, M. *Chem. Mater.* **2003**, *15*, 4139.

(5) Williams, D. J. *Angew. Chem., Int. Ed. Engl.* **1984**, *23*, 690.

(6) Nalwa, H. S.; Watanabe, T.; Miyata, S. In ref 1b, p 89.

(7) Dagani, R. *Chem. Eng. News* **1996**, March 4, 22.

10.1021/cm060584p CCC: $33.50
Published on Web 07/06/2006

Scheme 2

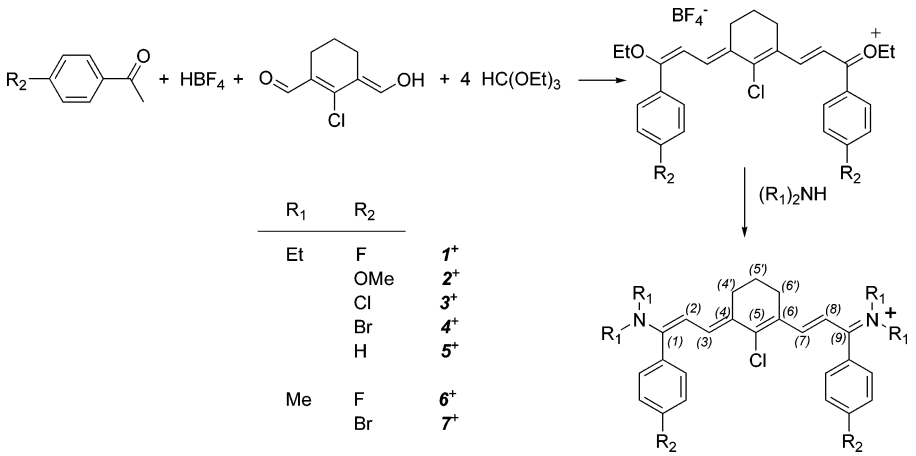

R_1	R_2	
Et	F	$\mathbf{1}^+$
	OMe	$\mathbf{2}^+$
	Cl	$\mathbf{3}^+$
	Br	$\mathbf{4}^+$
	H	$\mathbf{5}^+$
Me	F	$\mathbf{6}^+$
	Br	$\mathbf{7}^+$

growth of chromophores into noncentrosymmetric spaces groups, which leads to spontaneous acentric alignments and, hence, permanent macroscopic NLO response.[8]

In the present study, a few highly polarizable cationic chromophores are investigated, however with a modest "push−pull" electronic character and a charge strongly delocalized over the whole extent of the π-conjugated backbone. Their general molecular structure is shown in Scheme 2. Interestingly, some of these materials crystallize into noncentrosymmetric space groups, which favors charge localization on one end of the chromophores, by symmetry lowering, and finally restores a push−pull character in their electronic transitions and hence a sizable β value.

After the report of the synthesis and crystal structures, the optical and nonlinear optical properties will be computationally analyzed by semiempirical quantum procedures and experimentally by second harmonic generation (SHG) measurements performed on powdered samples.

Experimental Section

Starting Materials and Equipment. Compounds $\mathbf{2}^+(BF_4)^-$, $\mathbf{3}^+(BF_4)^-$, $\mathbf{4}^+(BF_4)^-$, $\mathbf{6}^+(BF_4)^-$, and $\mathbf{7}^+(BF_4)^-$ and reference 4′-dimethylamino-1-methylstilbazolium iodide ($DAMS^+I^-$) compound were synthesized as previously described.[9,10] Melting points were determined with a Büchi capillary apparatus. The UV−vis spectra were recorded on a Hewlett-Packard 8453 UV−vis spectrophotometer. Fluorescence spectra were recorded on a Perkin-Elmer LS 50B spectrofluorimeter equipped with a xenon-pulsed lamp (20 kW, flash time 8 μs) and a Hamamatsu R 928 photomultiplicator. Nuclear magnetic resonance spectra were obtained on a multinuclear Brücker AC250 spectrophotometer operating in the Fourier transform mode at 250.13 (^{1}H) or 62.89 (^{13}C) MHz. Mass spectra were obtained on a Nermag R10-10H apparatus in electrospray positive mode (CH_3CN). Elemental analysis was performed by the microanalysis service of the Laboratoire de Chimie de Coordination (LCC) in Toulouse.

Synthesis. *General Procedure*. To a solution of 0.73 mmol of the tetrafluoroborate carboxonium salt[9] in 20 mL of anhydrous acetonitrile was added 0.15 mL (1.45 mmol) of freshly distilled diethylamine. After being stirred for 24 h under an argon atmosphere at room temperature, the solution was filtered off. The solvent was then removed under reduced pressure, and the crude product was recrystallized from ethanol.

Data for 5-Chloro-1,9-bis(diethylamino)-1,9-bis(4-fluorophenyl)-4,6-[propane-1,3-diyl]nona-1,3,5,7-tetraenylium Tetrafluoroborate ($\mathbf{1}^+(BF_4)^-$). Green needles. Yield: 33%. Mp: 219 °C dec. ^{1}H NMR (250 MHz, CD_3CN, 25 °C) [δ (ppm), J (Hz)]: 1.19 (t, 12H, 7.3, $N(CH_2CH_3)_2$); 1.76 (quint, 2H, 6.1, $H_{5'}$); 2.52 (t, 4H, 6.1, $H_{4'-6'}$); 3.47 (m, 8H, $N(CH_2CH_3)_2$); 6.09 (d, 2H, 13.0, H_{2-8}); 6.98 (d, 2H, 13.0, H_{3-7}); 7.26 (m, 8H, H_{arom}). ^{13}C NMR (62.89 MHz, CD_3CN, 25 °C) [δ (ppm)]: 13.4 $(CH_3CH_2)_2N$); 21.7 ($C_{5'}$); 27.4 ($C_{4'-6'}$); 47.8 $(CH_3CH_2)_2N$); 107.1 (C_{2-8}); 116.7 ($^2J_{CF}$ = 22.6 Hz, CH_{arom}); 124.6 (C_{4-6}); 130.5 (C_{arom}-C_{1-9}); 131.9 (CH_{arom}); 149.8 (C_{3-7}); 150.0 (C_5-Cl); 163.9 (d, ^{1}J = 299.6, C_{arom}-F); 167.7 (C_{1-9}). MS (electrospray, positive mode, CH_3CN): $[M]^+$ at m/z (rel intens) 523.34 (100), 525.30 (41.7). Anal. Calcd for $C_{32}H_{38}BClF_6N_2$ (610.27): C, 62.91; H, 6.27; N, 4.59. Found: C, 62.99; H, 6.03; N, 4.45. UV−vis (23 °C, CH_2Cl_2): λ_{max} = 696 nm, ϵ_{max} = 248000 L mol^{-1} cm^{-1}, shoulder at 640 nm. Fluorescence (23 °C, CH_2Cl_2): $\lambda_{emission}$ = 726 nm.

Data for 5-chloro-1,9-diethylamino-1,9-diphenyl-4,6[propane-1,3-diyl]nona-1,3,5,7-tetraenylium Tetrafluoroborate ($\mathbf{5}^+(BF_4)^-$). Green needles. Yield: 15%. Mp: 222 °C dec. ^{1}H NMR (250 MHz, CD_3CN, 25 °C) [δ (ppm), J (Hz)]: 1.19 (t, 12H, 7.0, $N(CH_2CH_3)_2$); 1.76 (quint, 2H, 6.0, $H_{5'}$); 2.52 (t, 4H, 6.0, $H_{4'-6'}$); 3.46 (m, 8H, $N(CH_2CH_3)_2$); 6.09 (d, 2H, 13.3, H_{2-8}); 6.97 (d, 2H, 13.3, H_{3-7}); 7.23 (m, 4H, H_{arom}); 7.50 (m, 6H, H_{arom}). ^{13}C NMR (63 MHz, CD_3CN, 25 °C) [δ (ppm)]: 13.4 $(CH_3CH_2)_2N$); 21.7 ($C_{5'}$); 27.5 ($C_{4'-6'}$); 47.7 $(CH_3CH_2)_2N$); 106.8 (C_{2-8}); 124.3 (C_{4-6}); 129.4 (CH_{arom}); 129.7 (CH_{arom}); 130.8 (CH_{arom}); 134.3 (C_{arom}-C_{1-9}); 150.0 (C_{3-7} and C_5-Cl); 168.7 (C_{1-9}). MS (electrospray, positive mode, CH_3CN): $[M]^+$ at m/z (rel intens) 487.40 (100), 489.36 (44.0). Anal. Calcd for $C_{32}H_{40}BClF_4N_2$ (574.29): C, 66.85; H, 7.01; N, 4.87. Found: C, 66.39; H, 6.90; N, 5.14. UV−vis (23 °C, CH_2Cl_2): λ_{max} = 694 nm, ϵ_{max} = 280000 L mol^{-1} cm^{-1}, shoulder at 640 nm. Fluorescence (23 °C, CH_2Cl_2): λ_{em} = 717 nm.

Structure Analysis and Refinement. Crystal data for $\mathbf{1}^+(BF_4)^-$ and $\mathbf{5}^+(BF_4)^-$ were collected at 193 K using an oil-coated, shock-cooled crystal on a Bruker-AXS CCD 1000 diffractometer using Mo Kα radiation (λ = 0.71073 Å). Semiempirical absorption coefficients were employed.[11] The structure was solved by direct methods (SHELXS-97)[12] and refined using the least-squares method

(8) Prasad, P. N.; Williams, D. J. *Introduction to Nonlinear Optical Effects in Molecules and Polymers*; John Wiley & Sons: New York, 1991; p 132.

(9) (a) Izquierdo, A.; Guieu, V.; Gornitzka, H.; Madaule, Y.; Payrastre, C. *Eur. J. Org. Chem.* **2004**, 2317. (b) Guieu, V., Ph.D. Thesis, Université de Toulouse 3, 2005.

(10) Kung, T. K. *J. Chin. Chem. Soc.* **1978**, *25*, 131.

(11) *SADABS, Program for Data Correction*; Bruker-AXS: Madison, WI, 2001.

Table 1. Crystal Data for $1^+(BF_4)^-$ and $5^+(BF_4)^-$

	$1^+(BF_4)^-$	$5^+(BF_4)^-$
	Crystal Data	
empirical formula	$C_{32}H_{38}BClF_6N_2$	$C_{32}H_{40}BClF_4N_2$
mol wt	610.90	574.92
cryst size (mm)	0.4 × 0.2 × 0.05	0.6 × 0.6 × 0.2
cryst syst	monoclinic	orthorhombic
space group	$P2_1$	$P2_12_12_1$
a (Å)	13.481(1)	7.9731(5)
b (Å)	8.317(1)	13.703(1)
c (Å)	13.811(1)	28.139(2)
β (deg)	93.960(2)	90.0
V (Å^3)	1545.0(3)	3074.3(3)
ρ_{calcd} (Mg/m^3)	1.313	1.242
μ(Mo Kα) (cm^{-1})	0.184	0.172
	Data Collection	
radiation (Mo Kα) (Å)	0.71073	0.71073
scan mode	ϕ and ω	ϕ and ω
θ range (deg)	1.48−26.36	1.45−26.38
no. of reflns		
measured	9093	17942
unique	4958	6268
	Refinement	
refinement on	F^2	F^2
no. of variables	383	402
H atom treatment	mixed	mixed
R [I > 2σ(I)]	0.0461	0.0520
R_w	0.0758	0.1011
$\Delta\rho_{max}$ (e Å^{-3})	+0.233	+0.233
$\Delta\rho_{min}$ (e Å^{-3})	−0.200	−0.167
GOF	0.980	1.025

on F^2.[13] All non-hydrogen atoms were anisotropically refined, and in the last cycles of refinement a weighting scheme was used, where weights are calculated from the following formula: $w = 1/[\sigma^2(F_o^2) + (aP)^2 + bP]$, where $P = (F_o^2 + 2F_c^2)/3$. In the case of $\mathbf{5}^+(BF_4)^-$, a disorder was solved on the anion, with an occupancy of 0.56/0.44 for each fluorine atom. The crystallographic data are summarized in Table 1. Drawing of molecules was performed, with 50% probability displacement ellipsoids for non-hydrogen atoms. Crystallographic data have been deposited with the Cambridge Crystallographic Data Centre as supplementary publication nos. CCDC 600891 and 600892 for $\mathbf{1}^+(BF_4)^-$, and $\mathbf{5}^+(BF_4)^-$, respectively.

Theoretical Methods. The all-valence INDO (intermediate neglect of differential overlap) method,[14,15] in connection with the sum over states (SOS) formalism, was employed for the calculation of the electronic spectra and the molecular hyperpolarizabilities.[16] Details for the computationally efficient INDO−SOS-based method for describing molecular optical nonlinearities have been reported elsewhere.[17] In the present approach, the monoexcited configuration interaction (MECI) approximation was employed to describe the excited states. The lowest 100 energy transitions were chosen to undergo CI mixing. All calculations were performed using the INDO/1 Hamiltonian incorporated in the commercially available software package ZINDO.[18] Metrical parameters used for the calculations were those obtained from the present crystal structure determination.

NLO Measurements. The nonlinear optical properties were evaluated in the solid state as the efficiency in SHG expressed versus that of a reference (urea). The measurements were performed by the Kurtz−Perry powder technique[19] using a nanosecond Nd:YAG pulsed (10 Hz) laser operating at $\lambda = 1.064$ μm. The outcoming Stokes-shifted radiation at $\lambda = 1.907$ μm generated by the Raman effect in a hydrogen cell (1 m long, 50 atm) was used as the fundamental incident wavelength. The SHG signal was selected through a suitable interference filter, detected by a photomultiplier, and recorded on an ultrafast Tektronic TDS 620 B oscilloscope. Samples were powders obtained by grinding and put between two glass plates. They were calibrated in the 50−80 μm range. The thickness of the samples and references was 0.2 mm to keep the scattering effect in the same range of magnitude.

Results and Discussion

Design of Highly Polarizable Dyes. Polymethinium dyes are conjugated organic compounds containing a chain made up of an odd number of carbon atoms between two nitrogen atoms, one of which is positively charged. They are called cyanine dyes if both nitrogen atoms are included in conjugated heterocycles, hemicyanines if only one nitrogen belongs to a heterocycle (e.g., in DAMS$^+$), and streptocyanine otherwise. The present investigation is devoted to streptocyanine molecules, in which the highly delocalized electronic structure leads to various potential applications as dyes, photographic sensitizers, recordable laser disks, and fluorescent probes.[20]

In recent years, we have developed the synthesis of steptocyanines dyes from the reaction of pentacarbon,[21] heptacarbon,[22] and nonacarbon[9] chain carboxonium salts with various nitrogen nucleophiles. This allows the design of dyes in which the absorption wavelengths can be tuned across the visible and near-infrared spectrum by changing the length of the conjugated chain and the nature of the terminal substituents. The first motivation for the study of these new dyes is related to their fluorescence. This property is used, for example, to study the diffusion of single streptocyanine in the nanoporous network of sol−gel glasses.[23] A few years ago, we reported on the first NLO properties observed in pentamethinium derivatives.[24] In the present study, the investigation is extended to a series of nonacarbon chain derivatives, which lead to 6−7 times enhancement of the SHG efficiencies, in the more favorable case, versus the previously reported value (vide infra).

Nonacarbon chain streptocyanine dyes (e.g., $\mathbf{1}^+(BF_4)^-$ and $\mathbf{5}^+(BF_4)^-$) are obtained by nucleophilic substitution reaction

(12) Sheldrick, G. M. *Acta Crystallogr.* **1990**, *A46*, 467.
(13) Sheldrick, G. M. *SHELXL-97, Program for Crystal Structure Refinement*; University of Göttingen: Göttingen, Germany, 1997.
(14) Pople, J. A.; Beveridge, D. L.; Dobosh, P. A. *J. Chem. Phys.* **1967**, *47*, 2026.
(15) (a) Zerner, M.; Loew, G.; Kirchner, R.; Mueller-Westerhoff, U. *J. Am. Chem. Soc.* **1980**, *102*, 589. (b) Anderson, W. P.; Edwards, D.; Zerner, M. C. *Inorg. Chem.* **1986**, *25*, 2728.
(16) Ward, J. F. *Rev. Mod. Phys.* **1965**, *37*, 1.
(17) Kanis, D. R.; Ratner, M. A.; Marks, T. J. *Chem. Rev.* **1994**, *94*, 195.
(18) *ZINDO*, release 96.0; Molecular Simulations Inc.: Cambridge, U.K., 1996.
(19) (a) Kurtz, S. K.; Perry, T. T. *J. Appl. Phys.* **1968**, *39*, 3798. (b) Dougherty, J. P.; Kurtz, S. K. *J. Appl. Crystallogr.* **1976**, *9*, 145.
(20) (a) Mishra, A.; Behera, R. K.; Behera, P. K.; Mishra, B. K.; Behera, G. B. *Chem. Rev.* **2000**, *100*, 1973 and references herein. (b) Matsui, M.; Hashimoto, Y.; Funabiki, K.; Jin, J. Y.; Yoshida, T.; Minoura, H. *Synth. Met.* **2004**, *148*, 147. (c) Lin, Y.; Weissleder, R.; Tung, C. H. *Bioconjugate Chem.* **2002**, *13*, 605.
(21) Obaya, N.; Payrastre, C.; Madaule, Y. *Tetrahedron* **2001**, *57*, 9137 and reference herein.
(22) Izquierdo, A.; Payrastre, C.; Gornitzka, H.; Madaule *Eur. J. Org. Chem.* **2003**, 2370.
(23) Hellriegel, C.; Kirstein, J.; Bräuchle, C.; Latour, V.; Pigot, T.; Olivier, R.; Lacombe, S.; Brown, R.; Guieu, V.; Payrastre, C.; Izquierdo, A.; Mocho, P. *J. Phys. Chem. B* **2004**, *108*, 14699.
(24) (a) Lacroix, P. G.; Malfant, I.; Payrastre, C.; Wolf, J. G.; Bonvoisin, J.; Nakatani, K. *Chem. Mater.* **1998**, *10*, 1135. (b) Schanne-Klein, M. C.; Hache, F.; Roy, A.; Flytzanis, C.; Payrastre, C. *J. Chem. Phys.* **1998**, *108*, 9436.

Scheme 3

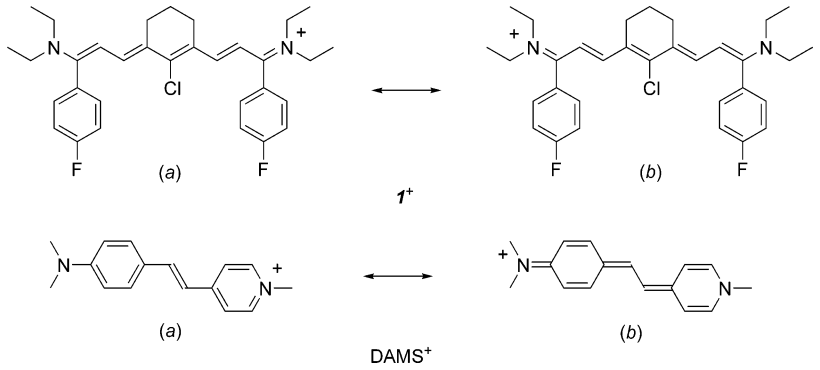

of the two ethoxy groups of the carboxonium tetrafluoroborate salts[9,25] with diethylamine (Scheme 2). The synthesis requires dry conditions to avoid degradation of the carboxonium salt. Once isolated, the streptocyanine dyes $\mathbf{1}^+(BF_4)^-$ and $\mathbf{5}^+(BF_4)^-$ can be handled without any precautions.

The NMR spectra clearly indicate the presence of a 2-fold symmetry axis for $\mathbf{1}^+$ and $\mathbf{5}^+$ in solution. In other words, the molecular ground state arises from an equal mixture of the two resonance forms (**a** and **b**), illustrated for cation $\mathbf{1}^+$ in Scheme 3. ^{1}H NMR spectra of $\mathbf{1}^+(BF_4^-)$ and $\mathbf{5}^+(BF_4^-)$ show $^3J_{H3-H7} = {}^3J_{H2-H8}$ coupling constants of 13 and 13.3 Hz, respectively, in agreement with an "*all-trans*" conjugated carbon chain. ^{13}C NMR shifts show that the carbon atoms C_1-C_9, C_3-C_7, and C_5 are deshielded (149.8 ppm $< \delta <$ 168.7 ppm) whereas C_2-C_8 and C_4-C_6 are more shielded (106.8 ppm $< \delta <$ 124.3 ppm). These observations can be interpreted as an alternate charge distribution, positive for C_1-C_9, C_3-C_7, and C_5 and negative for C_2-C_8 and C_4-C_6.

Structural Studies. Single crystals of $\mathbf{1}^+(BF_4)^-$ and $\mathbf{5}^+(BF_4)^-$ were grown from recrystallization in ethanol. It must first be emphasize that, in the case of $\mathbf{1}^+(BF_4)^-$, crystals of very large size ($\geq$1 mm) are easily obtained. This observation provides an additional interest as large crystals are usually greatly desirable for applications in nonlinear optics.

The molecular structure of $\mathbf{1}^+(BF_4)^-$ and atom labeling scheme are shown in Figure 1, and the crystal cell is shown in Figure 2. The compound crystallizes in the noncentrosymmetric monoclinic $P2_1$ space group. The crystal cell is built up from two molecules related by a 2_1 helicoidal symmetry axis. A careful examination of the molecular structure reveals that the two nitrogen atoms and the nine sp^2-hybridized carbon linkages lie in an almost perfect plane, with a largest distance of 0.082 Å observed from the mean plane at N2. This leads to the possibility of a strong charge delocalization along the 11-membered chain, according to the resonance equilibrium illustrated in Scheme 3. By contrast, the two aromatic rings are roughly perpendicular with respect to the π-conjugated molecular plane. Marks and Ratner have previously reported that twisted π-electron systems could lead to extremely large NLO responses in some cases.[26] However, this behavior occurs in chromophores with charge-separated zwitterionic ground states, which is not the case in the present $\mathbf{1}^+$ cation.

(25) Reynolds, G. A.; Drexhage, K. H. *J. Org. Chem.* **1977**, *42*, 885.

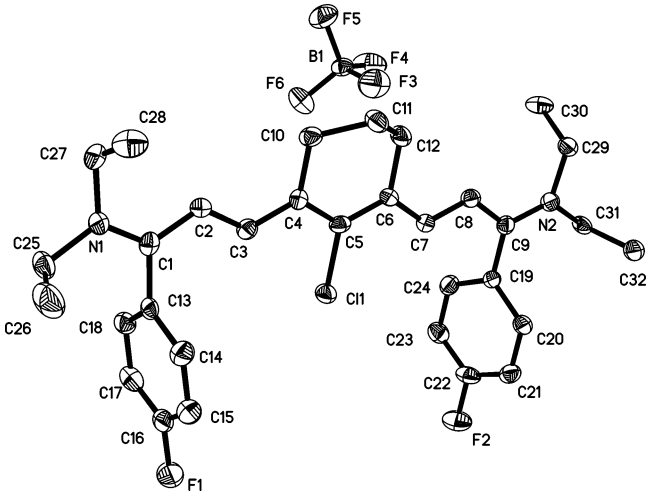

Figure 1. Asymmetric unit for compound $\mathbf{1}^+(BF_4)^-$ with atom labeling scheme. H atoms are omitted for clarity.

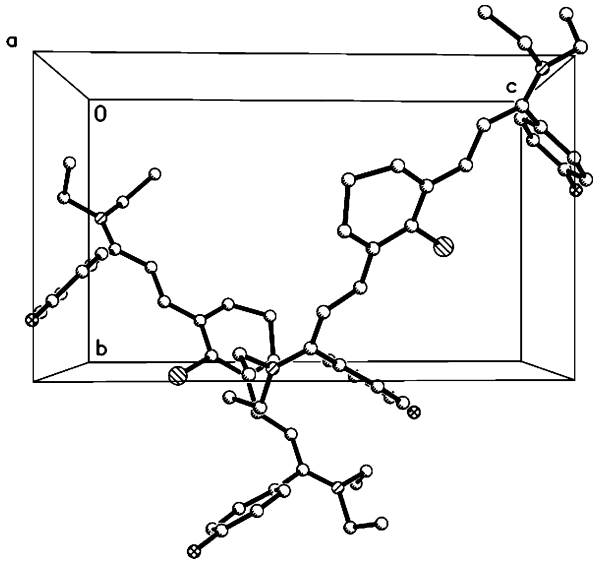

Figure 2. Crystal cell for $\mathbf{1}^+(BF_4)^-$ in the *bc* plane. The BF_4^- anions are omitted for clarity.

Molecule $\mathbf{5}^+(BF_4)^-$ crystallizes in the orthorhombic $P2_12_12_1$ space group, four molecules being present in the crystal cell, all of them related by a 2_1 symmetry axis. The asymmetric unit and atom labeling scheme are shown in Figure 3, and the crystal cell is shown in Figure 4. As observed in $\mathbf{1}^+(BF_4)^-$, the 11-membered chain lies in a plane, with a largest distance of 0.171 Å observed from the mean plane at C2.

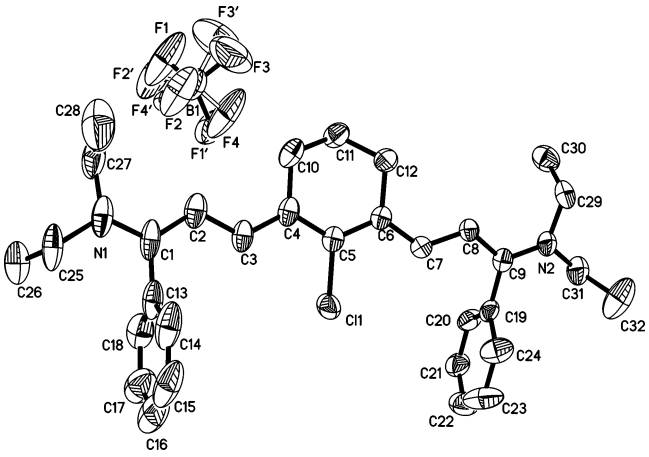

Figure 3. Asymmetric unit for compound $\mathbf{5}^{+}(BF_4)^{-}$ with atom labeling scheme. H atoms are omitted for clarity.

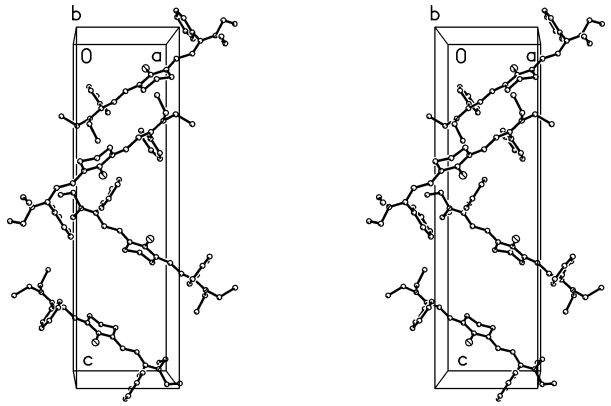

Figure 4. Crystal cell for $\mathbf{5}^{+}(BF_4)^{-}$ in the *ac* plane. The BF_4^{-} anions are omitted for clarity.

Table 2. Spectroscopic Data (λ_{max}, nm; ϵ, mol^{-1} L cm^{-1}) Recorded in CH_2Cl_2 for Compounds $\mathbf{1}^{+}(BF_4)^{-}$ to $\mathbf{7}^{+}(BF_4)^{-}$

compd	λ_{max}	ϵ	compd	λ_{max}	ϵ
$\mathbf{1}^{+}(BF_4)^{-}$	696	248000	$\mathbf{5}^{+}(BF_4)^{-}$	694	280000
$\mathbf{2}^{+}(BF_4)^{-}$	698	254000	$\mathbf{6}^{+}(BF_4)^{-}$	694	220000
$\mathbf{3}^{+}(BF_4)^{-}$	698	269000	$\mathbf{7}^{+}(BF_4)^{-}$	697	230000
$\mathbf{4}^{+}(BF_4)^{-}$	699	275000			

Optical Spectroscopy and Solvatochromism. The UV−vis spectroscopic data recorded in CH_2Cl_2 for compounds $\mathbf{1}^{+}(BF_4)^{-}$ to $\mathbf{7}^{+}(BF_4)^{-}$ are gathered in Table 2.[9b] The spectra are dominated by intense ($\epsilon \geq 200000$ mol^{-1} L cm^{-1}) transitions, having absorption maxima located between 694 and 699 nm. These similarities support the idea that the optical properties are related to the 11-membered conjugated chain, as anticipated from the examination of the X-ray data available. In any cases, the spectra recorded in solution reveal a surprisingly narrow band, with a nearly perfect optical transparency in the 200−550 nm range. This behavior is exemplified for $\mathbf{1}^{+}(BF_4)^{-}$ in Figure 5, where the optical spectrum of $DAMS^{+}I^{-}$ is drawn as a reference. $DAMS^{+}$ is a widely investigated NLO cation, which has occasionally provided extremely efficient NLO materials.[27] $DAMS^{+}$

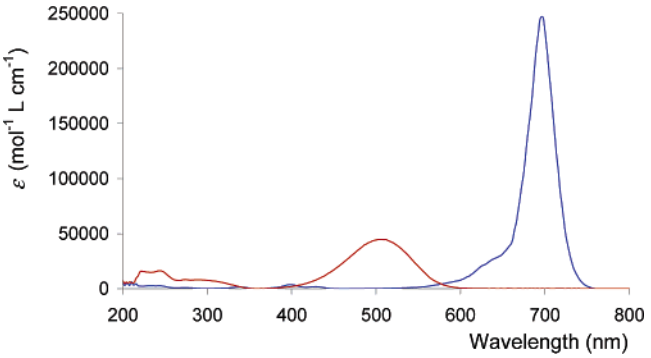

Figure 5. UV−vis spectrum in CH_2Cl_2 for $\mathbf{1}^{+}(BF_4)^{-}$ (blue) with that of $DAMS^{+}I^{-}$ (red) recorded as a reference.

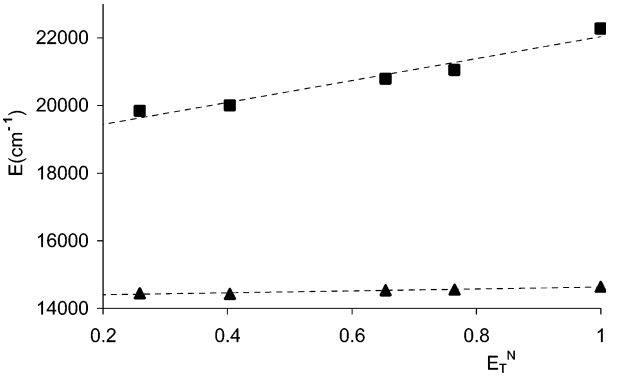

Figure 6. Energy maxima for the intense optical transition of $\mathbf{1}^{+}(BF_4)^{-}$ (triangles) and $DAMS^{+}I^{-}$ (squares) as a function of the Reichardt solvent polarity constant (E_T^N).

exhibits an intense charge-transfer transition (bandwidth of 3450 cm^{-1}), together with several additional bands of reduced intensity at higher energy. By contrast, the spectrum of $\mathbf{1}^{+}$ possesses a single and very narrow band (bandwidth of 780 cm^{-1}) and an extended range of transparency in the UV range, a highly desirable optical feature when NLO properties have to be considered.

The spectroscopic data recorded in solvents of different polarities for both $\mathbf{1}^{+}(BF_4)^{-}$ and $DAMS^{+}I^{-}$ are drawn in Figure 6 as a function of the Reichardt polarity constant (E_T^N),[28] used as an empirical solvent parameter.[9b] As is well-known, solvatochromism (a change in transition energy induced by a solvent polarity change) is usually indicative of dipole moment changes ($\Delta\mu$) upon electronic transition and hence large molecular hyperpolarizabilities (vide infra). By contrast versus $DAMS^{+}I^{-}$, $\mathbf{1}^{+}(BF_4)^{-}$ exhibits a very small solvatochromic shift, with a reduction of the slope from 3240 to 270 on passing from $DAMS^{+}I^{-}$ to $\mathbf{1}^{+}(BF_4)^{-}$.

To rationalize this effect, it must be remembered that the electronic ground state of π-conjugated chromophores arises from a combination of two resonance forms, namely, **a** and **b** in Scheme 3. $DAMS^{+}$ exhibits a strong push−pull character originated in the aminopyridinium conjugated structure. This implies that form **a** is dominant in the ground state and form **b** is dominant in the excited state, with the outcome of an intense charge transfer ($\Delta\mu$) arising upon $\pi \rightarrow \pi^*$ electronic transition. By contrast, the symmetry observed in the π-electronic structure of $\mathbf{1}^{+}$ implies a ground

(26) (a) Kang, H.; Facchetti, A.; Zhu, P.; Jiang, H.; Yang, Y.; Cariati, E.; Righetto, S.; Ugo, R.; Zuccaccia, C.; Macchioni, A.; Stern, C. L.; Liu, Z.; Ho, S. T.; Marks, T. J. *Angew. Chem., Int. Ed.* **2005**, *44*, 7922. (b) Albert, I. D. L.; Marks, T. J.; Ratner, M. A. *J. Am. Chem. Soc.* **1998**, *120*, 11174.

(27) Marder, S. R.; Perry, J. W.; Schaefer, W. P. *Science* **1989**, *245*, 626.

(28) Reichard, C.; Harbuch-Görnet, E. *Liebigs Ann. Chem.* **1983**, *5*, 721.

Table 3. Powder Efficiencies in Second Harmonic Generation Recorded at 1.907 and 1.064 μm for Compounds $1^+(BF_4)^-$ to $7^+(BF_4)^-$

	SHG			SHG	
compd	1.907 μm	1.064 μm	compd	1.907 μm	1.064 μm
urea[a]	1	1	$\mathbf{4}^+(BF_4)^-$	0	0
$\mathbf{1}^+(BF_4)^-$	120	100	$\mathbf{5}^+(BF_4)^-$	70	45
$\mathbf{2}^+(BF_4)^-$	0	0	$\mathbf{6}^+(BF_4)^-$	0	0
$\mathbf{3}^+(BF_4)^-$	0	0	$\mathbf{7}^+(BF_4)^-$	0	0

[a] Reference.

Table 4. Molecular Hyperpolarizabilities ($\beta_{total} = \beta_{2level} + \beta_{3level}$) and Angles between β_{total} and β_{2level} for $1^+(BF_4)^-$ and $5^+(BF_4)^-$

	wavelength (μm)	β_{total} (10^{-30} cm^5 esu^{-1})	β_{2level} (10^{-30} cm^5 esu^{-1})	β_{3level} (10^{-30} cm^5 esu^{-1})	angle (deg) (β_{total} vs β_{2level})
$\mathbf{1}^+(BF_4)^-$	∞	104.3	134.1	53.1	22
	1.907	188.3	230.4	72.1	16
$\mathbf{5}^+(BF_4)^-$	∞	67.3	67.6	35.8	30
	1.907	112.9	115.3	48.8	25

state described by a 1:1 mixture of the two resonance forms **a** and **b** presented in Scheme 3, as anticipated from the molecular symmetry and the previous discussion of the NMR data. Therefore, $\mathbf{1}^+(BF_4)^-$ likely lacks the strong push−pull character (large $\Delta\mu$ value) required for a large β value in solution.

Nonlinear Optical Properties. The efficiencies in SHG are reported in Table 3 for $\mathbf{1}^+(BF_4)^-$, $\mathbf{2}^+(BF_4)^-$, $\mathbf{3}^+(BF_4)^-$, $\mathbf{4}^+(BF_4)^-$, $\mathbf{5}^+(BF_4)^-$, $\mathbf{6}^+(BF_4)^-$, and $\mathbf{7}^+(BF_4)^-$. Most of the samples exhibit zero efficiency in relation to a possible crystal centrosymmetry. By contrast, and despite the absence of "push−pull" electronic character in solution, anticipated from the NMR and solvatochromic behavior, unusually large signals equal to 120 and 70 times that of urea are observed in the case of $\mathbf{1}^+(BF_4)^-$ and $\mathbf{5}^+(BF_4)^-$, respectively. These intriguingly large NLO responses have motivated (i) an X-ray crystal structure determination to verify the crystallization of the chromophores in noncentrosymmetric space groups and (ii) a computational investigation to find a rationale toward the microscopic origin of the optical nonlinearities.

Details for the β calculation of $\mathbf{1}^+(BF_4)^-$ and $\mathbf{5}^+(BF_4)^-$ are provided in Table 4. Within the SOS approach, β is related to all excited states of a molecule and can be partitioned into two components, so-called two-level (β_{2level}) and three-level (β_{3level}) terms.[17] In the present case, it clearly appears that β_{2level} dominates the nonlinearity, β_{3level} being reduced and directed into another direction different from that of β. Therefore, it can readily be assumed that β is qualitatively described by the two-level term, which relates the NLO response to the optical transitions according to the following relation:[29]

$$\beta_{2level} = \sum_i \frac{3e^2\hbar f_i \Delta\mu_i}{2mE_i^3} \frac{E_i^4}{(E_i^2 - (2\hbar\omega)^2)(E_i^2 - (\hbar\omega)^2)} \quad (1)$$

In this equation, f_i, $\Delta\mu_i$, and E_i are the oscillator strength, the difference between the ground- and excited-state dipole moments, and the energy of the ith transition, respectively ($\hbar\omega$ being the energy of the incident laser beam). The data gathered in Table 5 show that the low-lying $1 \rightarrow 2$ electronic transition is the only one to contribute significantly to β_{2level} (90.9% and 87.5% of the effect for $\mathbf{1}^+(BF_4)^-$ and $\mathbf{5}^+(BF_4)^-$, respectively). Furthermore, this transition is deeply HOMO−LUMO based in both cases, leading to the conclusion that understanding the charge transfer associated with the HOMO → LUMO excitation provides the rationale for the understanding of the NLO response. As the same qualitative behaviors are observed for the two dyes, the results will be precisely discussed in the next section for $\mathbf{1}^+(BF_4)^-$ only.

Table 5. Energy (λ_{max}, nm), Oscillator Strength (f), Dipole Moment Change ($\Delta\mu$, D) between Ground and Excited States, Contribution (%) in β_{2level}, and Composition of the Dominant Excited State Involved in the NLO Response of $1^+(BF_4)^-$ and $1^+(BF_4)^-$

transition	λ_{max}	f	Dm	state percent[a]	composition[b] of CI expansion
			$\mathbf{1}^+(BF_4)^-$		
$1 \rightarrow 2$	581	2.12	4.4	90.9	$0.962\chi_{98\rightarrow99}$
			$\mathbf{5}^+(BF_4)^-$		
$1 \rightarrow 2$	578	2.15	2.9	87.5	$0.964\chi_{92\rightarrow93}$

[a] Contribution of the transition in β_{2level}. [b] Orbital 98 is the HOMO and 99 the LUMO for $\mathbf{1}^+(BF_4)^-$. Orbital 92 is the HOMO and 93 the LUMO for $\mathbf{5}^+(BF_4)^-$.

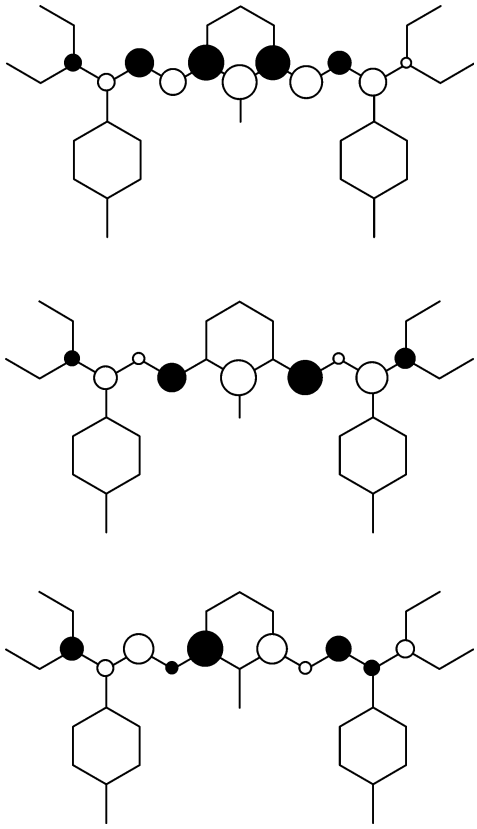

Figure 7. Frontier orbitals, HOMO (bottom) and LUMO (middle), for $\mathbf{1}^+(BF_4)^-$ with charge transfer associated with the HOMO → LUMO transition (top). White (black) contributions are indicative of an increase (decrease) in electron density in the charge-transfer process.

The frontier orbitals of cation $\mathbf{1}^+$ and the associated charge transfer are shown in Figure 7. At first glance, the electron density is symmetrically shared on the π-conjugated skeleton of the molecule at both the HOMO and LUMO levels. Nevertheless, the calculation of the charge-transfer process ($LUMO^2 - HOMO^2$ at the top of Figure 7) reveals that the

(29) (a) Oudar, J. L. *J. Chem. Phys.* **1977**, *67*, 446. (b) Oudar, J. L.; Chemla, J. *J. Chem. Phys.* **1977**, *66*, 2664.

symmetry lowering induced by the crystal noncentrosymmetry restores a push−pull effect and a sizable charge transfer to the 1 → 2 transition ($\Delta\mu = 4.4$ D, Table 5). This leads to a surprisingly large β value of 188.3×10^{-30} cm^5 esu^{-1} at the 1.907 μm laser wavelength.

On passing from molecular to bulk NLO properties, it has to be remembered that the SHG efficiency requires the molecules to be engineered in noncentrosymmetric solid-state environments (e.g., $P2_1$ and $P2_12_12_1$ in the case of $\mathbf{1}^+(BF_4)^-$ and $\mathbf{5}^+(BF_4)^-$, respectively). However, the fact that a chromophore crystallizes in a noncentrosymmetric space group does not guarantee that the molecular packing is optimized for NLO purposes. Therefore, the structure−property relationships have to be investigated to evaluate the potential efficiency of the present molecular materials.

In the solid state, the hyperpolarizability tensor (component β_{ijk} in the molecular framework) is related to the corresponding crystalline first-order nonlinearity tensor $\chi^{(2)}$ (component d_{IJK} in the crystalline framework).[30] Assuming a one-dimensional character of the molecular tensor (which is totally justified in the present case), β has only one large coefficient along the charge-transfer axis x of the molecule (namely, β_{xxx}). In the monoclinic $P2_1$ space group ($\mathbf{1}^+(BF_4)^-$), this leads to the following relations:[31,32]

$$d_{ZXX} \propto \beta_{xxx} \cos\theta \sin^2\theta$$

$$d_{ZZZ} \propto \beta_{xxx} \cos^3\theta$$

All other components of the tensor are weak (θ is defined as the angle between the resulting molecular charge-transfer axis Ox and the 2-fold axis OZ of the crystal). The optimization of d_{ZZZ} can be achieved with $\theta = 0°$, a situation which is of no practical use, for reasons related to the absence of phase matching capability. More importantly, the angular factor weighting β_{xxx} in the expression of d_{ZXX} is maximized and equal to 0.385 for $\theta = 54.7°$. Any situation emphasizing this coefficient is therefore valuable. In the case of $\mathbf{1}^+(BF_4)^-$, it is important to point out that θ is precisely equal to 54.0°. The structure is therefore perfectly optimized for this material.

In the case of the orthorhombic $P2_12_12_1$ space group ($\mathbf{5}^+(BF_4)^-$), the only nonvanishing component of $\chi^{(2)}$ is then

$$d_{XYZ} \propto \beta_{xxx} \sin\phi \cos\phi \cos\theta \sin^2\theta$$

where ϕ and θ are angular parameters defined by the Euler spherical angles.[30] For this space group, the optimized angular factor weighting d_{XYZ} is equal to 0.192. In the case of $\mathbf{5}^+(BF_4)^-$, the crystal data provide angular values of 43.6° and 86.0° for ϕ and θ, respectively. This leads to an angular factor equal to 0.035, therefore much lower than the 0.385 value calculated for $\mathbf{1}^+(BF_4)^-$. It is therefore not surprising that the crystal efficiency is far reduced in $\mathbf{5}^+(BF_4)^-$ versus that of $\mathbf{1}^+(BF_4)^-$.

Zyss et al. have extended this approach to any noncentrosymmetric space group.[30] They have found that the more promising space groups are those deriving from point group 2 (e.g., $P2_1$). These crystals are those in which the largest angular factor values can be obtained (=0.385). This is precisely the situation encountered in $\mathbf{1}^+(BF_4)^-$. We therefore conclude that the present efficiency of 120 times that of urea is the largest NLO response accessible in the solid state for $\mathbf{1}^+$ in the present molecular conformation.

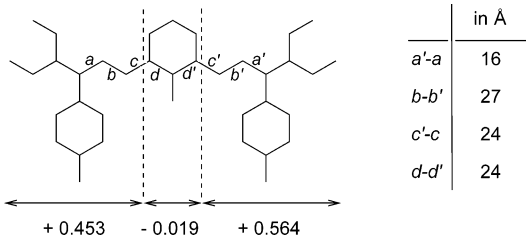

Figure 8. Mulliken populations and structural asymmetry (difference in equivalent i and i' bond lengths) in dye $\mathbf{1}^+$.

To further evaluate the potentiality of this family of π-conjugated streptocyanine dyes with nonacarbon chains, a final issue has to be addressed, related to the optimization of the β value accessible with the present π-electronic core. The differences in the conjugated carbon−carbon bond lengths, labeled as i and i', with respect to the pseudosymmetry of the chromophore are shown in Figure 8 for $\mathbf{1}^+$. While bond lengths i and i' are equivalent in solution, the solid-state geometry reveals an averaged difference of 0.023 Å in favor of an increased weight for resonance form **a** (Scheme 3). Furthermore, the Mulliken population supports the assumption that form **a** contributes only a little more than form **b** to the electronic ground state of $\mathbf{1}^+$.

On the basis of computational investigations, Marder et al. have suggested that the optimization of the molecular hyperpolarizability needs a special degree of mixing between the two resonance structures of a polymethine chain.[33] The difference between the average single and double carbon−carbon bond lengths is a good parameter to evaluate the "push−pull" character, called BLA (bond length alternation). Interestingly, they found that the largest β value is obtained for BLA = 0.055 Å.[34] In the case of dye $\mathbf{1}^+$, we calculate a BLA value equal to 0.023 Å, which suggests that the electron delocalization is still too important for optimizing the molecular NLO response. This seems not to be accessible with a symmetrically substituted streptocyanine, whatever the degree of charge localization by symmetry lowering in the solid state. We are currently trying to extend the synthetic approach to nonacarbon chains built up from different (e.g., EtO−, R_2N−) substituents to enlarge their intrinsic push−pull character, their molecular hyperpolarizabilities, and hopefully their solid-state efficiencies.

Conclusion

A family of pseudosymmetric cationic dyes has been reported which presents the rather surprising potential to lead

(30) Zyss, J.; Oudar, J. L. *Phys. Rev. A* **1982**, *26*, 2028.
(31) Oudar, J. L.; Zyss, J. *Phys. Rev. A* **1982**, *26*, 2016.
(32) Zyss, J.; Nicoud, J. F.; Coquillay, M. *J. Chem. Phys.* **1984**, *81*, 4160.
(33) Marder, S. R.; Beratan, D. N.; Cheng, L. T. *Science*, **1991**, *252*, 103.
(34) (a) Marder, S. R.; Gorman, C. B.; Tiemannn, B. G.; Cheng, L. T. *Proc. SPIE* **1993**, *1775*, 19. (b) Marder, S. R.; Gorman, C. B.; Tiemannn, B. G.; Cheng, L. T. *J. Am. Chem. Soc.* **1993**, *115*, 3006.

to highly SHG efficient molecular materials (up to 120 times the efficiency of urea). This large NLO response arises from the crystallization, which (i) enlarges the hyperpolarizability by loss of molecular symmetry and (ii) leads to an optimized tensor orientation in the solid state. These rigid molecules exhibit very good transparencies over an important optical range (between 200 and 550 nm) where most molecular NLO materials usually are highly absorbent. Additionally, the optimized compound $\mathbf{1}^{+}(BF_4)^{-}$ is easily accessible as single crystals of large size (around 1 mm).

Supporting Information Available: X-ray crystallographic data for $\mathbf{1}^{+}(BF_4)^{-}$ and $\mathbf{5}^{+}(BF_4)^{-}$. This material is available free of charge via the Internet at http://pubs.acs.org. Data have been deposited with the Cambridge Crystallographic Data Centre: CCDC 600891 and CCDC 600892.

CM060584P